JACS JOURNAL OF THE AMERICAN CHEMICAL SOCIETY

Communication

pubs.acs.org/JACS

Superconducting Fiber with Transition Temperature up to 7.43 K in $Nb_2Pd_xS_{5-\delta}$ (0.6 < x <1)

Hongyan Yu,[†] Ming Zuo,[‡] Lei Zhang,[†] Shun Tan,[‡] Changjin Zhang,*[,†,‡] and Yuheng Zhang[†,‡]

[†]High Magnetic Field Laboratory, Chinese Academy of Sciences and University of Science and Technology of China, Hefei 230026, People's Republic of China

[‡]Hefei National Laboratory for Physical Sciences at Microscale, University of Science and Technology of China, Hefei 230026, People's Republic of China

Supporting Information

ABSTRACT: Wiring systems powered by highly efficient superconductors have long been a dream of scientists, but researchers have faced practical challenges such as finding flexible materials. Here we report superconductivity in $Nb_2Pd_xS_{5-\delta}$ fibers with transition temperature up to 7.43 K, which have typical diameters of 0.3–3 μm. Superconductivity occurs in a wide range of Pd (0.6 < x <1) and S (0 < δ <0.61) contents, suggesting that the superconductivity in this system is very robust. Long fibers with suitable size provide a new route to high-power transmission cables and electronic devices.

Exploring new superconducting materials has long been a topic of interest in condensed matter physics and material science communities as well as industrial field. Cuprate superconductors[1] and iron-based superconductors[2] are two kinds of particularly important superconducting materials among the hundreds of superconducting materials discovered up to now. The highest superconducting transition temperature (T_c) at ambient pressure can be 132 and 56 K for cuprate superconductors and iron-based superconductors, respectively. Some high-temperature superconductors have become practically applicable in recent years. For example, high-quality superconducting wires based on $YBa_2Cu3O_{7-\delta}$ and $Bi_2Sr_2CaCu_2O_8$ superconductors have been fabricated for demonstrations of superconducting magnets, transmission cables, motors and other electrical power components.[3] However, these superconducting materials are both ceramic, so that they are difficult to be shaped. For practical uses, it is very important that a superconducting material is flexible. In recent years, new superconducting compounds, such as $BaTi_2Sb_2O$, $Bi_4O_4S_3$, $Nb_2Pd_{0.81}S_5$, $Nb_3Pd_{0.7}S_7$, Li_2Pd_3B, $LaNiGa_2$, and Ir_xCh_2 (Ch = Se and Te) are discovered.[4−11] Despite the relatively lower superconducting transition temperature (<10 K), their discovery attracts much attention due to their potential application perspectives and scientific importance. Here we report the growth and the characterization of $Nb_2Pd_xS_{5-\delta}$ (0.6 < x < 1) superconducting fibers by using traditional flux-melting method. The fibers have typical diameters of 0.3–3 μm. The T_c value can be 7.43 K in $Nb_2Pd_{0.963}S_{4.967}$. It is found that within a wide range of Pd-site and S-site occupancy rates (0.6 < x < 1, δ < 0.61) the $Nb_2Pd_xS_{5-\delta}$ fibers exhibit superconducting transition, suggesting the superconductivity in $Nb_2Pd_xS_{5-\delta}$ fibers is very robust.

Figure 1a shows a typical scanning electron microscopy (SEM) image of the as-grown fibers. They are cylindrical in shape and the length can be as long as 4 cm (Figures S1 and S2). Figure 1b gives the SEM image of a single fiber. The

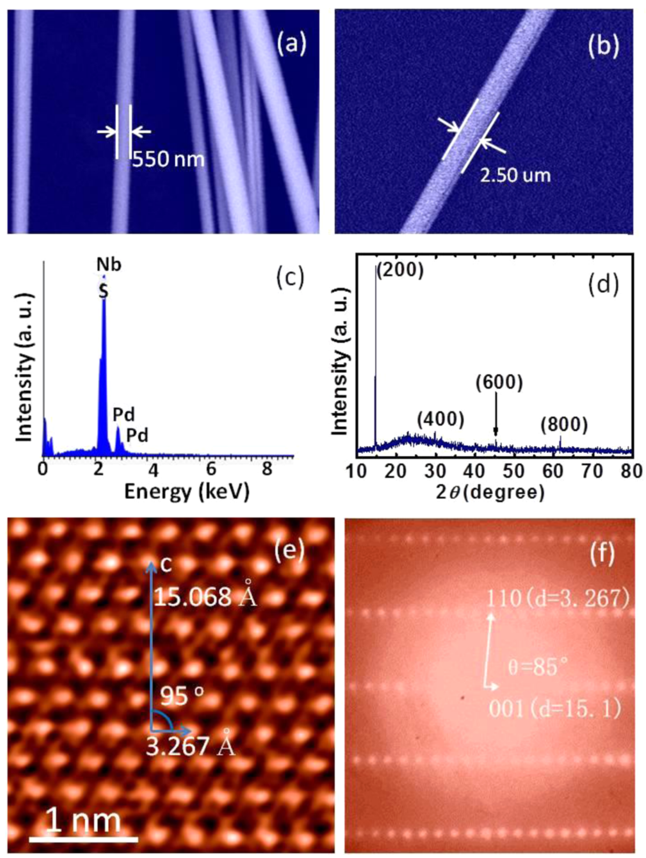

Figure 1. Crystal structure and chemical content. (a,b) SEM images of the as-grown fibers and a single fiber, respectively. (c) The EDX spectrum of a single fiber. (d) XRD pattern of the as-grown fibers. (e) Atomic-resolution TEM image of the fiber taken along the [1$\bar{1}$0] zone-axis direction. (f) HRTEM electron diffraction pattern of (e).

Received: June 20, 2013
Published: August 21, 2013

diameter of the fiber shown in Figure 1b is about 2.5 μm. It is found that these fibers can easily be bent into any shape, suggesting that they are flexible. In order to determine the chemical contents of the fibers, we perform an energy dispersive X-ray spectroscopy analysis (EDX) on these samples. The EDX spectrum (Figure 1c) confirms the presence of Nb, Pd, and S. A comparison between the starting compositions and the actual compositions of the fibers grown under different conditions is listed in Table S1. As can be seen from Table S1, excess S is added in the starting materials in order to compensate the evaporation at high temperature. It should be noticed that the occupancy rate of Pd is generally less than 1, meaning that there is some Pd-site vacancy in the fibers. From the chemical analysis we also notice that there is a certain vacancy at the S-site.

X-ray diffraction patterns of the as-grown $Nb_2Pd_xS_{5-\delta}$ ($0.6 < x < 1$) fibers (Figure 1d) taken on the surface of the cylinder confirm the single crystal behavior of the fiber. We notice that the chemical formula of $Nb_2Pd_xS_{5-\delta}$ is very similar to that of previous-discovered $Nb_2Pd_{0.71}S_5$ and $Nb_3Pd_{0.72}Se_7$.[12,13] Using the same monoclinic $C2/m$ space group and similar lattice parameters we find that the diffraction peaks shown in Figure 1d can be indexed to the diffraction from the ($l00$) planes. And the a-axis lattice constant is determined to be 12.041 Å. From the atomic-resolution tunneling electron microscopy (TEM) image and the high-resolution tunneling electron microscopy (HRTEM) electron diffraction pattern (Figures 1e,f and S3) results the b- and c-axis lattice constants are determined to be 3.396 and 15.068 Å, respectively.

Figure 2 gives the temperature dependence of electrical resistivity ($\rho\sim T$ curve) of the $Nb_2Pd_{0.963}S_{4.967}$ fiber. The $\rho\sim T$ curve is measured on one single fiber by using four-probe method. At high temperature, the $\rho\sim T$ curve exhibits metallic-like behavior. Clear resistivity drop can be observed below $T_c \approx$ 7.43 K. In order to verify that this resistivity drop is originated from superconducting transition, we perform measurements of magnetic susceptibility on the fibers. Figure 3 gives the temperature dependence of magnetic susceptibility of the $Nb_2Pd_{0.963}S_{4.967}$ superconducting fiber. At the high-temperature region, the magnetic susceptibility slightly increases with decreasing temperature without showing any signature of magnetic phase transition. Below ~7.2 K, diamagnetic signal presents, indicating the occurrence of superconducting transition. It can be seen that the superconducting transition width is less than 2 K, suggesting the high quality of the fiber. The $\rho\sim T$ curves measured under magnetic field suggest that the transport upper critical field is strongly dependent on the diameter of the fiber (Figure S4, the lower right inset of Figure 2). The fibers with smaller diameter exhibit higher upper critical field. Similarly, the critical current density (J_c) exhibits the same dependence on the diameter of the fiber (Figure S5). These facts suggest that both the transport upper critical field and J_c can be substantially enhanced by decreasing the diameter of the fiber.

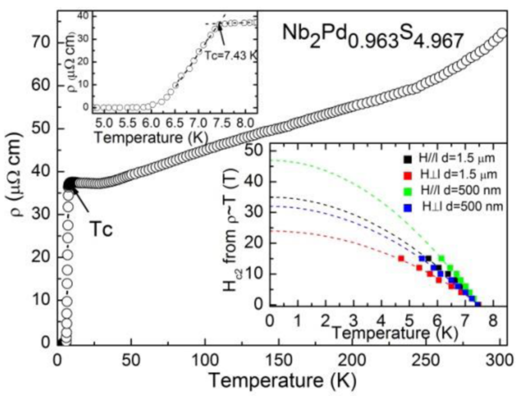

Figure 2. Temperature dependence of resistivity of the $Nb_2Pd_{0.963}S_{4.967}$ fiber. The upper-left inset shows an enlarged view near the transition temperature. The inset at lower right corner gives the upper critical field determined from the magneto-transport measurements. The dashed curves are the fitting data using $H_{c2}(T) = H_{c2}(0)\{1 - (T/T_c)^2\}$.

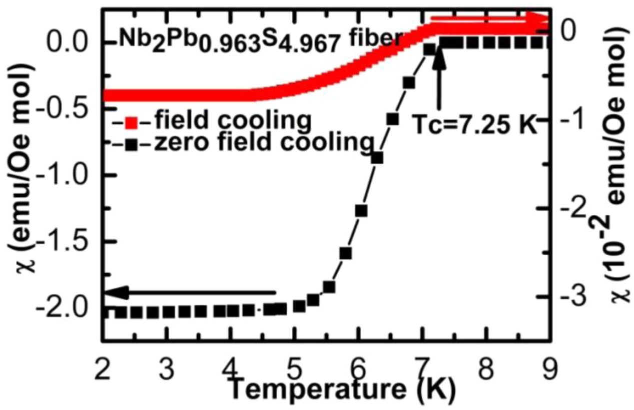

Figure 3. Temperature dependence of magnetic susceptibility of the $Nb_2Pd_{0.963}S_{4.967}$ fiber measured under both zero field cooling and field cooling processes. The inset shows the magnetic susceptibility at the high-temperature region.

We compare the T_c values for the samples prepared using different growth conditions and different starting compositions (Table S1). We find that both slow-cooling process and quenching method can yield superconducting fibers. The fibers prepared by quenching method exhibit higher transition temperature compared with those prepared by slow-cooling process. Furthermore, it is found that the fibers grown at 800 °C (the maximum temperature) followed by quenching down to room temperature exhibit higher T_c value. The Pd-site occupancy rate can be adjusted by changing the initial Pd content in the starting materials. Generally, we can obtain higher Pd-site occupancy rate if we add more Pd in the nominal composition. Table S1 suggests that the Pd-site occupancy rate varies from 0.6 to 1. It is interesting to notice that all $Nb_2Pd_xS_{5-\delta}$ ($0.6 < x < 1$, $0 < \delta < 0.62$) fibers exhibit superconducting transition, indicating that the superconductivity in this system is quite robust. The vacancy at the Pd- and S-sites is reminiscent of the K- and Fe-site vacancy in the $K_xFe_{2-y}Se_2$ superconductor.[14] However, the role of the Pd- and S-site vacancy in the occurrence of superconductivity in the $Nb_2Pd_xS_{5-\delta}$ fibers needs further investigation.

Figure 4 shows the magnetic hysteresis loop of the $Nb_2Pd_{0.963}S_{4.967}$ fiber measured at 2 K. The $M\sim\mu_0H$ curve of a typical type-II superconductor is observed. The lower critical field (H_{c1}), defined as the field at which the $M\sim\mu_0H$ curve deviates from the initial linear slope, is 39 Oe at 2 K. The upper critical field (H_{c2}) at 2 K is about 10.5 T (105 000 Oe). According to Ginzburg–Landau (GL) theory, the lower and upper critical fields at 0 K can be deduced using $H_c(T) = H_c(0)[1 - (T/T_c)^2]$. Thus the $H_{c1}(0)$ and $H_{c2}(0)$ values are

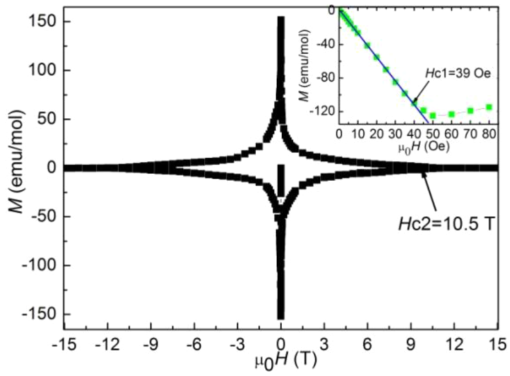

Figure 4. Magnetic field dependence of magnetic susceptibility of the $Nb_2Pd_{0.963}S_{4.967}$ fiber measured at 2 K. The green curve gives the initial $M \sim \mu_0 H$ isotherm. The blue line gives a linear fitting at the low-field region.

42.3 and 113 200 Oe, respectively. The GL parameter $\kappa(0)$ is estimated to be 76 using the equation $H_{c2}(0)/H_{c1}(0) = 2\kappa(0)^2/\ln \kappa(0)$.[15]

The GL coherence length at 0 K ($\xi(0)$), estimated using $\xi(0) = \{\Phi_0/[2\pi H_{c2}(0)]\}^{1/2}$, is about 5.4 nm. And the GL penetration depth $\lambda(0)$ is 410 nm based on the equation $\kappa(0) = \lambda(0)/\xi(0)$. It should be noted that the $\lambda(0)$ value is comparable with the diameters of the $Nb_2Pd_xS_{5-\delta}$ superconducting fibers, resulting in the fact that magnetic field can nearly completely penetrate through the fiber samples. In this sense, the $Nb_2Pd_xS_{5-\delta}$ fibers can serve as a possible candidate material to accurately measure the penetration depth.

In conclusion, we have found that superconductivity with T_c up to 7.43 K occurs in $Nb_2Pd_xS_{5-\delta}$ single crystal fibers. Within a wide range of Pd ($0.6 < x < 1$) and S ($0 < \delta < 0.62$) contents the fibers exhibit superconducting transition, suggesting that the superconductivity in this system is rather robust. The present results demonstrate that it is possible to fabricate flexible superconducting fibers for industrial applications.

■ ASSOCIATED CONTENT

Ⓢ Supporting Information

Experimental details, synthesis conditions of $Nb_2Pd_xS_{5-\delta}$ ($0.6 < x < 1$) fibers, and supporting table and figures. This material is available free of charge via the Internet at http://pubs.acs.org.

■ AUTHOR INFORMATION

Corresponding Author

zcjin@ustc.edu.cn

Notes

The authors declare no competing financial interest.

■ ACKNOWLEDGMENTS

This work was supported by the State Key Project of Fundamental Research of China (Grant Nos. 2010CB923403 and 2011CBA00111), the Nature Science Foundation of China (Grant Nos. 11174290 and U1232142), and the Hundred Talents Program of the Chinese Academy of Sciences.

■ REFERENCES

(1) Bednorz, J. G.; Müller, K. A. *Z. Phys. B* **1986**, *64*, 189−193.
(2) Kamihara, Y.; Watanabe, T.; Hirano, M.; Hosono, H. *J. Am. Chem. Soc.* **2008**, *130*, 3296−3297.
(3) Foltyn, S. R.; Civale, L.; MacManus-Driscoll, J. L.; Jia, Q. X.; Maiorov, B.; Wang, H.; Maley, M. *Nat. Mater.* **2007**, *6*, 631−642.
(4) Doan, P.; Gooch, M.; Tang, Z.; Lorenz, B.; Möller, A.; Tapp, J.; Chu, C. W.; Guloy, A. M. *J. Am. Chem. Soc.* **2012**, *134*, 16520−16523.
(5) Togano, K.; Badica, P.; Nakamori, Y.; Orimo, S.; Takeya, H.; Hirata, K. *Phys. Rev. Lett.* **2004**, *93*, 247004.
(6) Singh, S. K.; Kumar, A.; Gahtori, B.; Shruti; Sharma, G.; Patnaik, S.; Awana, P. S. *J. Am. Chem. Soc.* **2012**, *134*, 16504−16507.
(7) Zhang, Q.; Li, G.; Rhodes, D.; Kiswandhi, A.; Besara, T.; Zeng, B.; Sun, J.; Siegrist, T.; Johannes, M. D.; Balicas, L. *Sci. Rep.* **2013**, *3*, 1446.
(8) Zhang, Q. R.; Rhodes, D.; Zeng, B.; Besara, T.; Siegrist, T.; Johannes, M. D.; Balicas, L. *Phys. Rev. B* **2013**, *88*, 024508.
(9) Mizuguchi, Y.; Fujihisa, H.; Gotoh, Y.; Suzuki, K.; Usui, H.; Kuroki, K.; Demura, S.; Takano, Y.; Izawa, H.; Miura, O. *Phys. Rev. B* **2012**, *86*, 220510R.
(10) Hillier, A. D.; Quintanilla, J.; Mazidian, B.; Annett, J. F.; Cywinski, R. *Phys. Rev. Lett.* **2012**, *109*, 097001.
(11) Guo, J.; Qi, Y.; Matsuishi, S.; Hosono, H. *J. Am. Chem. Soc.* **2012**, *134*, 20001−20004.
(12) Keszler, D. A.; Ibers, J. A. *J. Am. Chem. Soc.* **1985**, *107*, 8119−8127.
(13) Keszler, D. A.; Ibers, J. A.; Shang, M. Y.; Lu, J. X. *J. Solid State Chem.* **1985**, *57*, 68−81.
(14) Guo, J.; Jin, S.; Wang, G.; Wang, S.; Zhu, K.; Zhou, T.; He, M.; Chen, X. *Phys. Rev. B* **2010**, *82*, 180520R.
(15) Tinkham, M. *Introduction to Superconductivity*, 2nd ed.; McGraw-Hill: New York, 1996.